Static balancing of an inverted pendulum with prestressed torsion bars

Radaelli, G.; Buskermolen, R.; Barents, R.; Herder, J. L.

DOI
10.1016/j.mechmachtheory.2016.10.005

Publication date
2017

Document Version
Accepted author manuscript

Published in
Mechanism and Machine Theory

Link to formal publication (Elsevier):
http://dx.doi.org/10.1016/.mechmachtheory.2016.10.005

Static balancing of an inverted pendulum with prestressed torsion bars

G. Radaelli[a,c], R. Buskermolen[b], R. Barents[c], J.L. Herder[a]

[a] *Dept. Precision and Microsystems Engineering, Delft University of Technology, Delft, The Netherlands*
[b] *Holland Container Innovations Nederland B.V., Rotterdamseweg 183-C, Delft, The Netherlands*
[c] *InteSpring B.V., Molengraaffsingel 12-14, Delft, The Netherlands*

Abstract

This paper presents a method for the design of a statically balanced inverted pendulum. The non-linear moment-rotation characteristic of the pendulum's weight is approximated by a piecewise linear characteristic. Each transition is realized by engaging or disengaging one or more torsion bars, by means of mechanical stops. The whole set of torsion bars is located along the hinge axis of the pendulum. A prototype with three parallel torsion bars was built. Experimental evaluation of the prototype revealed a 99% work reduction of the balanced pendulum with respect to the unbalanced one.

Keywords: static balancing, torsion springs, torsion bars, series spring, parallel springs

---

1. Introduction

In order to alleviate the operating forces of mechanical devices, it is possible to apply static balancing to counteract the weight of the system and/or its payload [1]. The result is a more manageable device in the case that it is human-operated, and less powerful actuators in the case that the device is powered. Other advantages of static balancing include intrinsic safety [2], intuitive man-machine interaction [3, 4], backlash reduction due to presstress, and weight reduction of motors and brakes [5]. Because of these advantages static balancing of weight has been proposed in numerous applications, especially in the fields of robotics [6, 7, 8, 9, 10], orthotics and assistive devices [11, 12, 13], and consumer products [14].

Most static balancing techniques involve the use of counter-masses [15], which have the disadvantage of increasing the overall mass and inertia of the system. A common alternative is to use extension springs [1], which have the disadvantage that the volume they occupy increases when the spring is loaded. In addition, most spring-based balancing techniques rely on the use of a special

Email addresses: g.radaelli@tudelft.nl (G. Radaelli), R.Buskermolen@hcinnovations.nl (R. Buskermolen), Rogier@intespring.nl (R. Barents), j.l.herder@tudelft.nl (J.L. Herder)

type of spring, namely a zero-free-length spring (ZFLS), which is not a common off-the-shelf component. Some authors have presented ways to circumvent the need for ZFLS proposing alternative balancing methods that are based on conventional springs with non-zero free-length [16, 17, 18, 19, 11].

Both kind of extension springs often have the disadvantage that the volume they occupy crosses the empty space between the elements of the device, which implies that the space is not available for other purposes. Think for example of an application where static balancing is to be applied in a foldable structure, such as a foldable sea container [20], to compensate the weight of the members of the structure. If there were extension springs crossing the free space inside the structure, this space would not be available for goods. Therefore more compact solutions that solely occupy space near the hinges are sought.

Koser [21] present a cam mechanism in combination with a compression spring that is designed as a compact unit at the base of a robotic manipulator. However, the assessment of the practical applicability of the concept is not completed up to the level of component design and physical evaluation. In practice, the high forces on the cam system combined with the very small design space may reveal as the limiting factors.

Shieh [22] presents a balancing mechanism that does not cross the free space by applying a Scotch Yoke spring mechanism which can be integrated within the link. Friction in the sliding parts are probably affecting the performance of balancing significantly, but the authors make no mention of this possible issue.

The employment of torsion springs at the hinges of a linkage would eliminate the named disadvantages. Torsion springs, namely, act at the point of rotation between two bodies and thus do not elongate when loaded. Very little work has been found that includes torsion springs for the purpose of balancing weights.

Gopalswamy [5] balances the weight of a parallelogram linkage with a single torsion spring with a linear characteristic. The range where the balance applies, however, is limited to the part of the sine characteristic that can be approximated as linear.

Trease [23] developed a gravity balanced four-bar linkage. An optimization procedure was used to obtain a constant potential energy of the masses and the open-cross compliant joints, a type of torsional springs. As the authors state, the presented solution is a specific one limited to the given parameter set only. A similar result was obtained by Radaelli [24], who developed a general design method for approximate static balancing of linkages with torsion springs. In one of the examples, a pendulum is balanced by an additional double link, obtaining in fact a four bar linkage with a balanced weight. In both cases the links that are added to balance the pendulum occupy a considerable amount of space. Therefore, in this regard, these solutions do not offer enough advantage with respect to the helical spring balancers.

In the present paper the case is considered of a body, modelled by a point mass connected by a weightless link to a revolute joint in an inverted pendulum arrangement, representing, e.g., a side wall of a foldable sea container. The pendulum moves over ninety degrees from the upright vertical position to a horizontal position. The weight will be balanced with torsion springs, namely torsion bars. Torsion bars have the advantage that they occupy approximately the same space loaded as unloaded. Moreover, normally the bars are situated at the hinge in the direction perpendicular to the plane of motion of the pendulum. This is especially advantageous for pendulums with large out-of-plane width, such as the side wall of the container.

Since normal torsion springs have a linear moment-angle characteristic, they can only linearly approximate the sinusoidal moment-angle characteristic of the weight. We propose the judicial employment of mechanical stops and prestress for the sequential activation or deactivation of different torsion bars in order to result in a piecewise linear moment characteristic. This piecewise linear characteristic can give better approximations of the nonlinear degressive characteristic of the weight.

Eshelman [25] describes an invention where a multi-rate torsion bar is employed for vehicle suspensions. An increased torsional stiffness is obtained with two serial torsion bars with one mechanical stop. Also Fader [26] describes a similar torsion bar for vehicle suspensions, where more mechanical stops are used to affect the total torsion stiffness of the bar. In his invention, Castrilli [27] obtains non-linearity in the torsion characteristic of a bar with a continuous contact profile along the length of the bar. This system can be regarded as an infinite number of bars of infinitesimal length in series, all with their own contact point.

All mentioned inventions concern torsion bars with increasing stiffness. A degressive stiffness, however, can only be obtained if the stops make contact initially, i.e. one or more bars are prestressed. Claus [28] designed such a system for static balancing of the walls of a foldable container. In a small-scale prototype he used a configuration of two serial torsion bars with one mechanical stop. No other examples of torsion spring systems with positive but degressive stiffness were found by the authors in literature.

The goal of this paper is to propose a method for balancing an inverted pendulum by a piecewise linear approximation of the nonlinear characteristic, obtained by the sequential (de-)activation of torsion springs. The design approach allows for unlimited number of linear segments. This number is only limited by the physical implementation of the torsion bars.

The outline of this paper is as follows. In section 2 the design methodology is described. Section 3 illustrates the design of the physical prototype, while in section 4 the testing procedure and the test results are provided. Finally a discussion and some conclusions can be found in sections 5 and 6, respectively.

2. Method

The present section starts with a description of the technical problem and of the conceptual solution. After that the design method will be discussed.

2.1. Problem Description

Consider the system depicted in Fig. 1a. A point mass m is attached to a weightless rigid link at a distance l from a hinge. The pendulum is allowed to move between its upright vertical position a, and 90 degrees clockwise, to the horizontal position b, thus $[a, b] = [0, \frac{\pi}{2}]$ rad. The weight of the pendulum produces a negative sinusoidal moment-angle characteristic at the hinge. Friction and other non-conservative forces are neglected. To maintain the system in equilibrium at every position, a system with a positive sinusoidal moment characteristic is needed to counteract the weight, see Fig. 1b. Focusing on the given range of motion it is required that the balancing system possesses a non-linear, positive and decreasing stiffness.

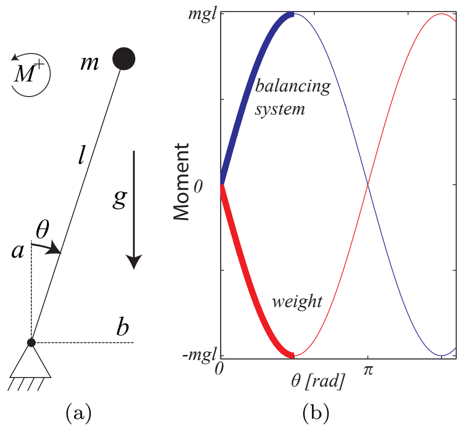

Figure 1: a) Inverted pendulum, b) moment-angle of pendulum and of ideal balancer.

A given design requirement is that the balancing system occupies as little space as possible around the hinge. In a sea container, the direction out of the plane of motion is along the hinge of the wall, thus along this hinge there is space available for the balancing system. This requirement practically excludes the employment of extension springs.

The high non-linearity and particularly the decreasing stiffness property makes it hard to think of solutions with normally employed torsion springs, since nearly all of those have a positive, maybe increasing stiffness.

2.2. Concept Solution

Obtaining a changing stiffness in a controlled manner can be done by the subsequent employment of more springs and mechanical stops. The mechanical stops serve to activate or deactivate a spring such to obtain a different compound of active springs, resulting in a non-constant stiffness, see [29]. The employed springs can be connected in series or in parallel or in a combination of both, as will be explained next.

Series - Assume two serial extension springs are fixed at one end and loaded at the other end, with a mechanical stop at the connection point of both springs, see Fig. 2a. The mechanical stop is not making contact. Increasing the applied load will cause the mechanical stop to make contact. Now one spring is allowed to deform further, while the other one keeps its current deformation and no longer contributes to the stiffness at the endpoint. The resulting stiffness is higher than before.

Series prestressed - Consider now the other way around. The same two springs are prestressed in such a way that the mechanical stop makes contact at the starting position, see Fig. 2b. One of the springs will initially not deform and therefore not contribute to the stiffness. Increasing the load will make the mechanical stop lose its contact when the load equals the prestress force. Now, both springs start to contribute to the stiffness, making the total stiffness lower than before.

Parallel - Analogous reasoning can be applied to parallel springs. Consider two parallel springs. One spring is connected to ground at one end and at a

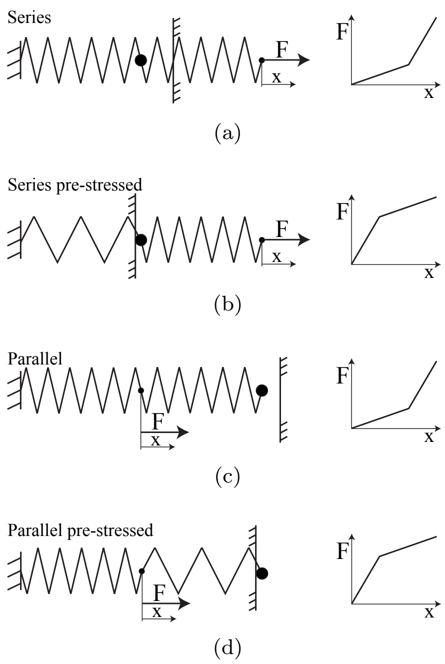

Figure 2: Variable stiffness with mechanical stops in extension springs. a) series making contact, b) prestressed series releasing contact, c) parallel making contact, d) prestressed parallel releasing contact.

common load point at the other end, and the other spring can be fixed or loose at one end due to the mechanical stop, and is connected to the load point at the other end, see Fig 2c. If the spring is unloaded initially, the total stiffness will increase when the mechanical stop makes contact.

Parallel prestressed - Consider the fourth case where the mechanical stop is initially active, thus there is a certain prestress force holding the contact. Once the load equals the prestress force the contact gets lose and second spring does not have any contribution to the stiffness. In fact, the second spring will have only a rigid-body motion from that point on. Since in parallel systems the stiffnesses add together, the result is a lower stiffness after contact is lost.

Extrapolating from this fundamental idea, it becomes possible to approximate different non-linear curves by piecewise-linear curves possibly involving two or more linear segments, obtained by one or more mechanical stops. The explanation with the extension springs, which is more easily illustrated, also holds for torsion springs or any other analogous situation with potential energy storage elements.

2.3. Design Method

The present subsection describes the linear approximation of the sine curve, that can be obtained by a single linear torsion spring for an approximate balance with a number of static equilibrium positions. It is followed by a description of the piecewise-linear approximation obtained by the passive (de-)activation of different prestressed linear torsion springs with mechanical stops. The result is an improved approximation of the sine curve with two static equilibrium points for every different spring.

2.3.1. Linear Approximation

Consider a single torsion spring, or any combination of springs, with a linear moment characteristic. If employed as balancing system for an inverted pendulum, the balance will always be approximate, and a certain number of static equilibrium positions can be obtained, depending on the energy function of the system to be balanced. The best fit between a linear segment and the segment of the sine depends on the choice of the objective function. For example, the maximum difference between both curves could be minimized to suppress high peak forces. Alternatively one could take the integral of the squared difference between both curves over the range of motion. This would lead to a lower work done over the whole range of motion. The choice is related to the application of the balanced system. With no real application at hand, in this paper the second objective is arbitrarily chosen. The dimensionless difference Δ between the sine and the line (normalized by amplitude $mgl = 1$) is given by

$$\Delta = \sin(\theta) - (K\theta + M) \tag{1}$$

where K is the slope of the line and M is the level of the line at $\theta = 0$. The objective is the integral of the squared difference over the range of motion, as

$$f = \min_{K,M} \int_a^b \Delta^2 d\theta \tag{2}$$

where K and M are varied to obtain the best fit. The optimization is performed with the aid of the Matlab® tool *slmengine*, which can perform a piecewise linear fitting to any dataset by least squares optimization.

The sine curve in the range $a = 0$, $b = \pi/2$, the fitted line and the resulting error curve are provided in Fig. 3. The optimized value for f is 0.0062. The optimized parameters K and M are 0.66 and 0.11, respectively. The system can be made with a torsional spring with stiffness $k = Kmgl$ and neutral angle

$$\alpha = -\frac{M}{K} \tag{3}$$

The maximum rotation which the spring undergoes is

$$\Theta = b - \alpha \tag{4}$$

2.3.2. Two-piece Linear Approximation

For an improved approximation the sine can be fitted with two linear segments, see Fig. 4. Both line segments can be described by their slopes K_1 and K_2, and their starting point defined by the coordinates θ_1, M_1, and θ_2, M_2. θ_1 is defined by the starting point of the range of motion a, in this case $\theta_1 = 0$. Moreover, M_2 is determined by the first line segment and the intersection angle θ_2. The set of parameters that remains available for the optimization are K_1, K_2, M_1 and θ_2. The dimensionless difference between the piecewise approximation and the sine is now given by

$$\Delta = \begin{cases} \sin(\theta) - (K_1\theta + M_1) & a \leq \theta < \theta_2 \\ \sin(\theta) - (K_2\theta + M_2) & \theta_2 \leq \theta < b \end{cases} \tag{5}$$

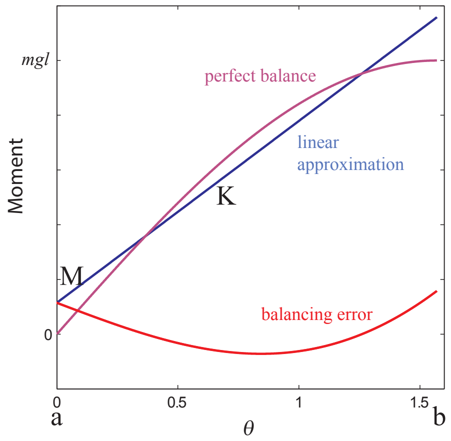

Figure 3: Linear approximation of perfect balancer, with balancing error.

and the objective becomes

$$f = \min_{K_1, K_2, M_1, \theta_2} \int_a^b \Delta^2 d\theta \tag{6}$$

The values that result from the optimization are

$$\begin{aligned}&[K_1, K_2, M_1, M_2, \theta_2] = \\ &\left[0.88 rad^{-1}, 0.32 rad^{-1}, 0.02, 0.83, 0.91 rad\right]\end{aligned} \tag{7}$$

and, given the range $a = 0$, $b = \pi/2$, the obtained value of the objective is $f = 3.2647e - 4$.

In a subsequent step, it is possible to choose whether to use two serial springs or two parallel springs.

Series springs

If both springs are in series, then in the first segment only one spring is active, and in the second segment also the other spring becomes active. The first spring thus must have the stiffness $k_1 = K_1 mgl$ and neutral angle $\alpha_1 = -\frac{M_1}{K_1}$ while the second spring has stiffness

$$k_2 = \frac{K_1 \cdot K_2}{K_1 - K_2} mgl \tag{8}$$

and neutral angle

$$\alpha_2 = -\frac{M_2 mgl}{k_2} \tag{9}$$

Parallel springs

In the case that the springs are parallel the stiffness of the first spring is

$$k_1 = (K_1 - K_2)\, mgl \tag{10}$$

while the stiffness of the second bar is simply $k_2 = K_2 mgl$. The neutral angles of the two springs are

$$\alpha_1 = \theta_2 \tag{11}$$

$$\alpha_2 = \theta_2 - \frac{M_2}{K_2} \tag{12}$$

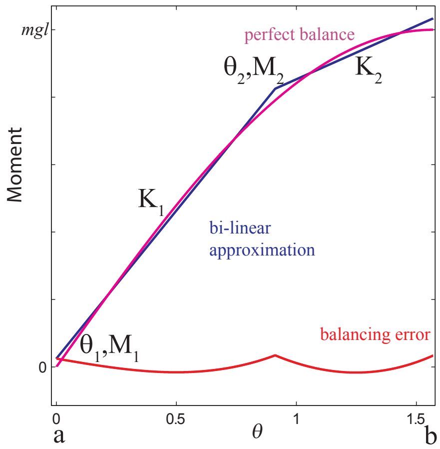

Figure 4: Bi-linear approximation of perfect balancer, with balancing error.

2.3.3. Multi-piece Linear Approximation

The procedure above can in principle be extended for any number of serial or parallel springs. Combinations of serial and parallel springs are also possible, but will not be considered here. For n number of linear segments, there are $2n$ free parameters to optimize. These are the slopes $K_1, K_2...K_n$, the height of the first intersection point M_1 and the angles of the following intersection points $\theta_2, \theta_3...\theta_n$, see Fig. 5. The difference function and the objective function are given by

$$\Delta = \begin{cases} \sin(\theta) - (K_1\theta + M_1) & a \leq \theta < \theta_2 \\ \sin(\theta) - (K_2\theta + M_2) & \theta_2 \leq \theta < \theta_3 \\ \vdots & \\ \sin(\theta) - (K_n\theta + M_n) & \theta_n \leq \theta < b \end{cases} \tag{13}$$

and

$$f = \min_{\mathbf{x}} \int_a^b \Delta^2 d\theta \tag{14}$$

with

$$\mathbf{x} = [K_1 \cdots K_n, M_1, \theta_2 \cdots \theta_n] \tag{15}$$

.

Series springs

In the case of a serial configuration, the spring parameters are obtained with

$$\begin{array}{ll} k_i = K_i mgl & i = 1 \\ k_i = \frac{K_{i-1} \cdot K_i}{K_{i-1} - K_i} mgl & i = 2...n \end{array} \tag{16}$$

$$\alpha_i = -\frac{M_i mgl}{k_i} \qquad i = 1...n \tag{17}$$

The maximum rotation undergone by the springs is

$$\Theta_i = \frac{M_b mgl}{K_i} \qquad i = 1...n \tag{18}$$

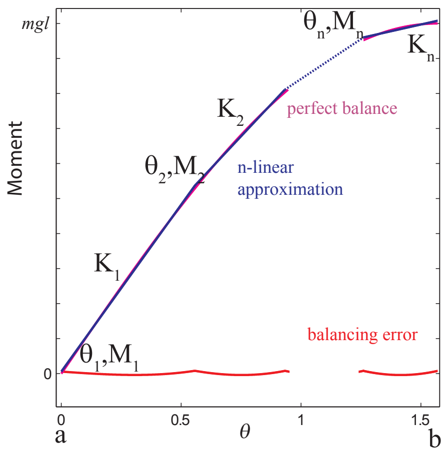

Figure 5: n-piece linear approximation of perfect balancer.

where M_b is the normalized moment at point b, that can be derived by

$$M_b = M_n + K_n \left(b - \theta_n\right) \tag{19}$$

Parallel springs

The spring parameters in the case of a parallel configuration of springs are obtained with

$$\begin{array}{ll} k_i = \left(K_i - K_{i+1}\right) mgl & i = 1...n-1 \\ k_i = K_i mgl & i = n \end{array} \tag{20}$$

$$\begin{array}{ll} \alpha_i = \theta_{i+1} & i = 1...n-1 \\ \alpha_i = \theta_i - \frac{M_i}{K_i} & i = n \end{array} \tag{21}$$

The maximum rotation undergone by the springs is

$$\begin{array}{ll} \Theta_i = \theta_i & i = 1...n-1 \\ \Theta_i = b - \alpha_i & i = n \end{array} \tag{22}$$

2.4. Number of bars

Evidently, the more linear segments are used, the better the approximation to the sine curve is. However, the advantage in fitting result may in practical cases not weight against the added complexity of a high number of springs. Therefore a trade-off should be made between complexity and accuracy, which is highly dependent on the intended application. Figure 6 shows the results of optimized objective function f as a function of the number of linear segments on a logarithmic scale. It can be observed that the advantage in accuracy is decreasing as the number of segments increases.

2.5. Choice between parallel and series

Also here, it is dependent on what the intended application of the balanced system is whether to prefer a serial configuration or a parallel one. However, some guidance can be found in the metric given next.

Considering that potential energy required to lift the pendulum does not change with the spring configuration, the sum of the maximum strain energy

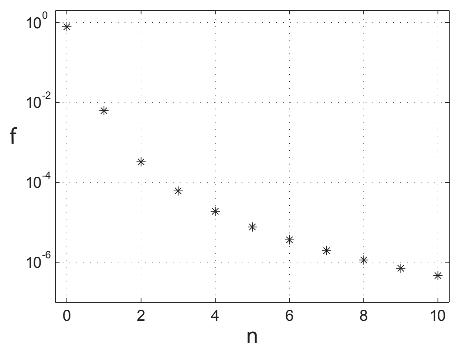

Figure 6: Result of optimization for different number of segments on logarithmic scale. Improvement in result is getting smaller as number of bars increases.

Nr. segments	1	2	3	4	5
series	1.01	1.69	2.48	3.29	4.11
parallel	1.01	1.92	2.82	3.69	4.54

Table 1: Sum of maximum strain energy in every bar, for different number of bars. Pendulum parameters are normalized to $mgl = 1$.

that is stored in the different springs separately can be used as an indicator for the efficiency of the system. The maximum energy storage U in the single springs is given by

$$U_i = \frac{1}{2} k_i \Theta_i^2 \tag{23}$$

and the sum of the strain energy over all springs is

$$U_{tot} = \sum_{i=1}^{n} U_i. \tag{24}$$

Table 1 gives some comparative values of total strain energy for series and parallel springs. It can be seen that the energy efficiency, as defined above, is worse for parallel systems because the energy metric is increasing faster w.r.t. serial systems.

3. Prototype

For the illustration and evaluation of the presented design approach, a prototype has been designed, constructed and tested. In the presented prototype, as an example for above mentioned possibilities, three parallel torsion bars are used to approximate static balancing of an inverted pendulum. The choice of three bars and the parallel configuration is arbitrary and is not related to the efficiency metric discussed above. A trilinear approximation of the first quarter-period of a sine function gives 2 orders of magnitude error reduction with respect to a linear approximation, see Fig. 6.

Parameter	units	value			
m, g, l	$[kg, ms^{-2}, m]$	5,	9.81,	0.5	
K_1, K_2, K_3	$[rad^{-1}]$	22.82,	14.79,	5.09	
a, θ_2, θ_3, b	$[rad]$	0,	0.68,	1.15,	1.57
M_1, M_2, M_3, M_b	$[-]$	0.26,	15.81,	22.74,	24.88
k_1, k_2, k_3	$[Nmrad^{-1}]$	8.03,	9.70,	5.09	
$\alpha_1, \alpha_2, \alpha_3$	$[rad]$	0.68,	1.15,	-3.32	
$\Theta_1, \Theta_2, \Theta_3,$	$[rad]$	0.68,	1.15,	4.89	
d_1, d_2, d_3	$[m]$	0.004,	0.005,	0.006	
L_1, L_2, L_3	$[m]$	0.247,	0.500,	1.975	

Table 2: Design parameters

3.1. Torsion bars

The spring type selected for this prototype are torsion bars. Torsion bars can occupy very narrow spaces along the hinge axis. Moreover, torsion bars have an efficient efficient energy storage per material volume as compared to springs that are loaded in bending [29], e.g., spiral springs and helical torsion springs.

For the dimensioning of torsion bars the material properties shear modulus G and maximum shear strength τ_{max} are needed. Given a circular cross-section of the bars, the length L_i and diameter d_i must satisfy the following relation in order to obtain the desired stiffness k_i

$$L_i = \frac{J_i G}{k_i} \tag{25}$$

where J is the polar moment of inertia, given by

$$J_i = \frac{\pi d_i^4}{32} \tag{26}$$

Moreover, as the maximum shear stress τ may not be exceeded, the following inequality must be satisfied

$$L_i \geq \frac{d_i G \Theta_i}{2\tau_{max}} \tag{27}$$

To use as little material as possible, one might want to chose the values for d and L for which this inequality is just fulfilled. However, for practical reasons, a round-off value of the diameter would be beneficial for the ease of purchasing the bar.

With the material properties $G = 79\ GPa$ and $\tau_{max} = 600\ MPa$ (alloy steel DIN 1.8159) the resulting design parameters are given in table 2.

The moment characteristic of the pendulum, the balancing system and both together are plotted in Fig. 7

3.2. Construction

A picture of the entire prototype is provided in Fig. 8. Some details of the construction are discussed next. The three bars have an L-shaped hook at one end, and are clamped in a common aluminium block in such a way to

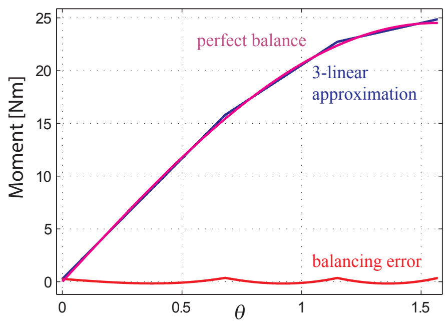

Figure 7: Three-Piece linear approximation for prototype.

impede relative rotation, see Fig 9a. This part is connected to a bearing and to the pendulum, with masses at adjustable distances. The longest torsion bar is positioned centrally with respect to the other two bars. It is assumed that the influence of the offset of the two short bars from the axis of rotation is negligible. At the free end of the two short bars a wing-shaped part is fixed. The wings can make contact with a perpendicular bolt at every side such to impede further rotation, see Fig. 9b. This system is the mechanical stop that makes the bar active only in a certain range of motion. Due to the bending stiffness of the bars it is not needed to support them at this end.

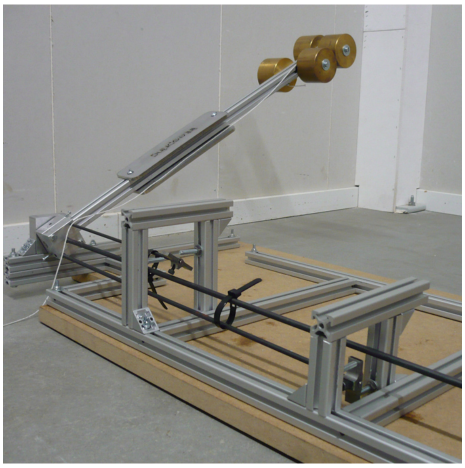

Figure 8: Picture of entire prototype. Three torsion bars with an arrangement of mechanical stops serve as gravity balancing system for an inverted pendulum.

4. Evaluation

The testing of the prototype and the results from the measurements are discussed in the present section. The mass of the pendulum and the distance of the centre of mass from the rotation axis, for which the best results were found experimentally, are

$$m_{real} = 5.0 \ kg \tag{28}$$

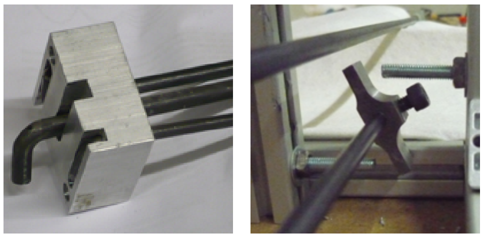

(a) (b)

Figure 9: Prototype details pictures. a) L-shaped bar ends clamped, b) mechanical stops, the wings touch the bolts impeding rotation from then on.

Nr	Stable/Unstable	Model [deg]	Prototype [deg]
1	U	9.3	4
2	S	31.8	38
3	U	45.1	43
4	S	60.4	60.5
5	U	71.0	69
6	S	84.9	84

Table 3: Equilibrium positions, prediction and measurements.

$$l_{real} = 0.487\ m \tag{29}$$

The distance is 0.013 m smaller than the optimized value.

4.1. Equilibrium positions

The system is expected to exhibit six equilibrium positions within the given range of motion, three stable ones and three unstable ones. The pendulum is positioned in proximity of the expected equilibrium positions. In the case of the stable equilibria, the system will spontaneously approach the state of equilibrium. In the case of unstable equilibria, the point is searched manually by feeling where the reaction force and the tendency to deviate from that position are minimal. Once the pendulum is positioned at these positions, the angle is measured with a bevel protractor. The results of this test are tabulated in table 3.

4.2. Moment-angle measurements

The next test aims to get a precise moment-angle characteristic of the prototype over the given range of motion. The measurements are performed with a vertical tensile bench. The load cell is connected by a wire to an aluminium disc with 30mm diameter. The disc, which is supported by a separate ball-bearing, is connected to the balancing system with a pin connection between the axis of the disc and the hollow axis of the balancing system. On the disc a counter-mass is attached through a wire over a pulley to make all forces tensile and thus measurable with this setup. This weight was later subtracted from the measurement result.
Two separate measurements are performed. One in which only the disc with the

mass and the pulley are connected, and one also including the pendulum with its balancing system. Subtracting both measurements from each other gives the moment contribution of the balanced pendulum. The measurements are performed two ways, from 0° to 90° and back from 90° to 0°. This way, a hysteresis loop is obtained. Taking the mean of the values for both directions at every angle gives an estimate of what the force would be in the absence of friction. This estimate is based on the assumption that the contribution of friction at every angle is equal in both directions. Figure 10 gives the measurements results of the measuring setup (red), the setup with the balanced pendulum (green) and the difference between both (blue). Also the mean value between the upper and lower part of the latest hysteresis loop is plotted (black), which is considered to be the moment coming from the balanced pendulum excluding friction. This moment-angle characteristic is compared to the modelled one in Fig. 11.

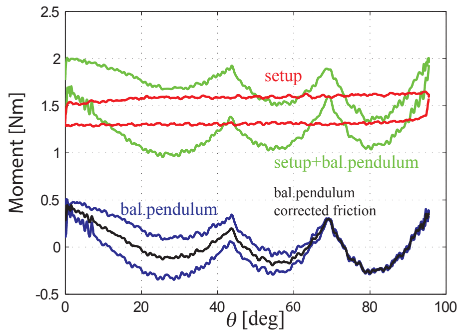

Figure 10: Moment-angle measurements. The measurements with the system and the measurements setup are corrected with measurements of the setup alone. The results are corrected for friction. The black line is considered to come from the balanced pendulum itself.

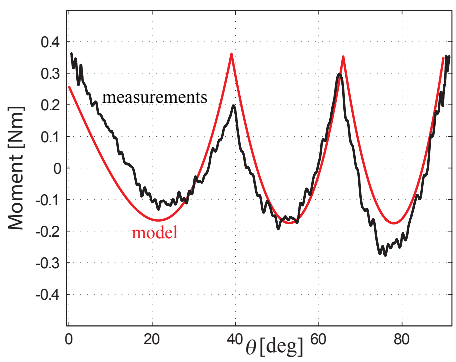

Figure 11: Measurements compared with the model. The resulting line from Fig 10 is plotted next to the error line of Fig 7

Two comparative parameters will be provided to evaluate the fit between the modelled curve and the measured curve: the root mean squared error $RMSE$ and the correlation coefficient ρ. These parameters, however, do not quantify the balancing quality. For this we take ratio R between the work done by the balanced pendulum over the work done by the unbalanced pendulum in one way over the range of motion.

$$R = \frac{W_{bal\ pendulum}}{W_{pendulum}} = \frac{W_{bal\ pendulum}}{g \cdot m_{real} \cdot l_{real}} \tag{30}$$

The results are

$$\begin{gathered} RMSE = 0.0868\ Nm \\ \rho = 0.8288 \end{gathered} \tag{31}$$

$$R = \frac{0.1996J}{23.8874J} = 0.0089 = 0.89\% \tag{32}$$

5. Discussion

5.1. Design approach

The discussed design approach based on a piece-wise linear approximation of a sine curve through multiple torsion bars with preload and mechanical stops seems to be a powerful and easy tool for the design of statically balanced inverted pendulums. The present design concerned a range of motion of 90 degrees. The design approach however, can be applied for different ranges of motion and potentially also for other types of non-linear moment characteristics. Yet it is not possible with springs with positive stiffness, to obtain a negative stiffness of the balancing system.

It is possible, but left for future work, to add the possibility of combining series and parallel springs together. This might be beneficial for the material and space-efficiency of the system. Also it must be investigated what type of non-linearities are possible to achieve. For example, is it possible to combine progressive and degressive slopes in one curve?

5.2. Measurements

The measurement results are quite satisfactory. The difference with the modelled results are small and qualitatively the behaviour is as expected. This can be verified with the number and location of the equilibria and the location of the transition points, i.e. where contact conditions change. The amount of work reduction of about 99% is also very satisfactory. About the measurements themselves, the amount of measured hysteresis is considered high. As seen in Fig. 10 however, most of the hysteresis stems from the measurements setup, the disc and pulley, and not from the balancing system. It is also noticed that significantly higher friction is present near the upright position of the pendulum. This is presumably the effect of misalignment of the bearings.

5.3. Material

The design of the balancing system is developed for a mass of 5 kg on a distance of 0.5 m. To obtain the best results in the prototype, however, a mass of 5 kg was fixed at a distance of 0.487 m. This difference of 2.6% is most probably due to variations in the shear modulus of the material. For employment of such a balancing mechanism in real-life applications either good tests beforehand should reveal the exact properties of the material, or the mechanism should be able to accommodate for adjustment of the torsional rigidity of the bars or one of the other design parameters.

5.4. Construction

The presented construction of the prototype revealed some interesting features:

- The absence of bearings for the two contacting bars combines a reduction in complexity and an improvement in terms of friction losses. In this case the bending stiffness of the bars suffices to sustain themselves and to guide themselves against the contacting points of the mechanical stops.
- The distance of the two short bars with respect to the axis of rotation does not compromise noticeably the energy accumulation properties of the bars, due to the low bending stiffness of the bars and the relatively small bending deflection of the bars during motion.

6. Conclusions

This paper presents the development of a design approach for static balancing of an inverted pendulum. The design approach is based on a piecewise linear approximation of the nonlinear moment characteristic of the pendulum, obtained with sequential (de)-activation of torsion springs using mechanical stops and pretension in a variety of arrangements. In the optimization procedure, the area between the original curve and the approximation is minimized, resulting in a system that requires minimal work for operation.

The design method is a tool to approximate balance with torsion springs in series and parallel configurations, up to an unlimited number of springs, limited only by physical construction constraints.

The method is used to approximate a sinusoidal curve, but can potentially be used for the approximation of other types of non-linear moment characteristics. For example, in a more complex linkage system subject to gravity, the effect of the weight can be translated into a needed moment characteristic at one or more hinges of the system.

A trilinear approximation of the first quarter-period of a sine function gives a factor 100 error reduction with respect to a linear approximation. A prototype with three parallel torsion bars was constructed and tested. As compared to the unbalanced pendulum, less then 1% of the work is needed to turn the pendulum 90° from upright to horizontal.

Acknowledgement

This research was carried out as part of SPISTA (SenterNovem kenniswerkersregeling, KWR09086) and ShellMech (STW HTSM-2012 12814).

[1] J. L. Herder, Energy-free Systems, Theory, conception and design of statically balanced spring mechanisms, PhD Thesis, Delft University of Technology, Delft, The Netherlands (November 2001).

[2] M. Vermeulen, M. Wisse, Intrinsically Safe Robot Arm: Adjustable Static Balancing and Low Power Actuation, International Journal of Social Robotics 2 (3) (2010) 275–288. doi:10.1007/s12369-010-0048-9.
URL `http://link.springer.com/10.1007/s12369-010-0048-9`

[3] V. Hayward, P. Gregorio, O. Astley, S. Greenish, M. Doyon, L. Lessard, J. McDougall, I. Sinclair, S. Boelen, X. Chen, others, Freedom-7: A high fidelity seven axis haptic device with application to surgical training, in: Experimental Robotics V, Springer, 1998, pp. 443–456.
URL http://link.springer.com/chapter/10.1007/BFb0112983

[4] R. Fan, C. Zhao, H. Zhao, Improvement of dynamic transparency of haptic devices by using spring balance, in: 2012 IEEE International Conference on Robotics and Biomimetics (ROBIO), 2012, pp. 1075–1080. doi:10.1109/ROBIO.2012.6491112.

[5] A. Gopalswamy, P. Gupta, M. Vidyasagar, A new parallelogram linkage configuration for gravity compensation using torsional springs, in: , 1992 IEEE International Conference on Robotics and Automation, 1992. Proceedings, 1992, pp. 664–669 vol.1. doi:10.1109/ROBOT.1992.220291.

[6] T. Rahman, R. Ramanathan, R. Seliktar, W. Harwin, A Simple Technique to Passively Gravity-Balance Articulated Mechanisms, Journal of Mechanical Design 117 (4) (1995) 655–658. doi:10.1115/1.2826738.
URL http://dx.doi.org/10.1115/1.2826738

[7] J. Wang, C. M. Gosselin, Static balancing of spatial three-degree-of-freedom parallel mechanisms, Mechanism and Machine Theory 34 (3) (1999) 437–452. doi:10.1016/S0094-114X(98)00031-7.
URL http://www.sciencedirect.com/science/article/pii/S0094114X98000317

[8] I. Simionescu, L. Ciupitu, The static balancing of the industrial robot arms: Part I: Discrete balancing, Mechanism and Machine Theory 35 (9) (2000) 1287–1298. doi:10.1016/S0094-114X(99)00067-1.
URL http://www.sciencedirect.com/science/article/pii/S0094114X99000671

[9] I. Simionescu, L. Ciupitu, The static balancing of the industrial robot arms: Part II: Continuous balancing, Mechanism and Machine Theory 35 (9) (2000) 1299–1311. doi:10.1016/S0094-114X(99)00068-3.
URL http://www.sciencedirect.com/science/article/pii/S0094114X99000683

[10] L. Kang, S.-M. Oh, W. Kim, B.-J. Yi, Design of a new gravity balanced parallel mechanism with Schnflies motion, Proceedings of the Institution of Mechanical Engineers, Part C: Journal of Mechanical Engineering Science (2015) 0954406215605862doi:10.1177/0954406215605862.
URL http://pic.sagepub.com/content/early/2015/09/29/0954406215605862

[11] A. Agrawal, S. K. Agrawal, Design of gravity balancing leg orthosis using non-zero free length springs, Mechanism and Machine Theory 40 (6) (2005) 693–709. doi:10.1016/j.mechmachtheory.2004.11.002.
URL http://www.sciencedirect.com/science/article/pii/S0094114X05000054

[12] A. G. Dunning, J. L. Herder, A review of assistive devices for arm balancing, in: 2013 IEEE International Conference on Rehabilitation Robotics (ICORR), 2013, pp. 1–6. doi:10.1109/ICORR.2013.6650485.

[13] B. Lenzo, M. Fontana, S. Marcheschi, F. Salsedo, A. Frisoli, M. Bergamasco, Trackhold: A Novel Passive Arm-Support Device, Journal of Mechanisms and Robotics 8 (2) (2015) 021007–021007. doi:10.1115/1.4031716.
URL http://dx.doi.org/10.1115/1.4031716

[14] M. J. French, M. B. Widden, The spring-and-lever balancing mechanism, George Carwardine and the Anglepoise lamp, Proceedings of the Institution of Mechanical Engineers, Part C: Journal of Mechanical Engineering Science 214 (3) (2000) 501–508. doi:10.1243/0954406001523137.
URL http://pic.sagepub.com/content/214/3/501

[15] H. Hilpert, Weight balancing of precision mechanical instruments, Journal of Mechanisms 3 (4) (1968) 289 – 302. doi:http://dx.doi.org/10.1016/0022-2569(68)90005-0.
URL http://www.sciencedirect.com/science/article/pii/0022256968900050

[16] J. M. Herve, Device for counter-balancing the forces due to gravity in a robot arm, u.S. Classification 414/720, 901/48, 700/900; International Classification B25J19/00, F16F15/28; Cooperative Classification Y10S700/90, B25J19/0016, F16F15/28; European Classification B25J19/00D4, F16F15/28 (Nov. 1986).
URL http://www.google.com/patents/US4620829

[17] D. A. Streit, B. J. Gilmore, Perfect Spring Equilibrators for Rotatable Bodies, Journal of Mechanisms, Transmissions, and Automation in Design 111 (4) (1989) 451–458. doi:10.1115/1.3259020.
URL http://dx.doi.org/10.1115/1.3259020

[18] N. Ulrich, V. Kumar, Passive mechanical gravity compensation for robot manipulators, in: , 1991 IEEE International Conference on Robotics and Automation, 1991. Proceedings, 1991, pp. 1536–1541 vol.2. doi:10.1109/ROBOT.1991.131834.

[19] F. L. S. te Riele, E. E. G. Hekman, J. L. Herder, Planar and Spatial Gravity Balancing With Normal Springs, ASME, 2004, pp. 415–424. doi:10.1115/DETC2004-57164.
URL http://proceedings.asmedigitalcollection.asme.org/proceeding.aspx?articleid=1651347

[20] G. Kusuma, J. Herder, Foldable container, EP Patent App. EP20,070,116,312 (Mar. 18 2009).
URL http://www.google.com/patents/EP2036835A1?cl=en

[21] K. Koser, A cam mechanism for gravity-balancing, Mechanics Research Communications 36 (4) (2009) 523–530. doi:10.1016/j.mechrescom.2008.12.005.
URL http://www.sciencedirect.com/science/article/pii/S0093641308001535

[22] W.-B. Shieh, B.-S. Chou, A Novel Spring Balancing Device on the Basis of a Scotch Yoke Mechanism, in: Proceedings of the 14th IFToMM World Congress, , 2015, pp. 206–212.
URL http://www.iftomm2015.tw/IFToMM2015CD/PDF/OS8-004.pdf

[23] B. Trease, E. Dede, Statically-Balanced Compliant Four-Bar Mechanism for Gravity Compensation, Ann Arbor 1001 (2004) 48109.
URL http://www-personal.umich.edu/~btrease/share/ASME2004/statically-balanced-4bar.pdf

[24] G. Radaelli, J. A. Gallego, J. L. Herder, An Energy Approach to Static Balancing of Systems With Torsion Stiffness, ASME Conference Proceedings 2010 (44106) (2010) 341–353. doi:10.1115/DETC2010-28071.
URL http://link.aip.org/link/abstract/ASMECP/v2010/i44106/p341/s1

[25] E. J. Eshelman, Multi-rate torsion bar independent suspension spring, Patent Application, US 2003/0201591 A1 (10 2003).
URL http://www.patentlens.net/patentlens/patent/US_2003_0201591_A1/en/

[26] J. Fader, M. Clements, C. Keeney, S. Yollick, J. Hawkins, Torsion bar with multiple arm adjusters for a vehicle suspension system, Patent, US 6425594 (07 2002).
URL http://www.patentlens.net/patentlens/patent/US_6425594/en/

[27] P. Castrilli, Nonlinear torsion spring, Patent, US 4884790 (12 1989).
URL http://www.patentlens.net/patentlens/patent/US_4884790/en/

[28] M. R. Claus, Gravity balancing using configurations of torsion bars; with application to the HCI foldable container, MS Thesis, Delft University of Technology, Delft, The Netherlands (December 2008).

[29] J. C. Cool, Werktuigkundige systemen, Vssd, Delft, The Netherlands, 2005.